# Western Region Technical Attachment
# No. 07-07
# May 31, 2007

## A RARE F-2 TORNADO EVENT IN BEAR, IDAHO

**Melissa M. Hurlbut**
*WFO Jacksonville, Florida (former affiliation WFO Boise, Idaho)*

ABSTRACT

Observational and model data were studied to assess the evolution of a significant microburst and tornado event in the Boise, Idaho, County Warning Forecast Area (CWFA). A squall line that formed ahead of a cold front (Fig. 1) produced damaging winds and severe hail across Baker County, in northeast Oregon. As the southern end of this squall line continued to evolve, an F2 tornado was spawned over Adams County, in southwest Idaho, which damaged structures, leveled trees across 2023 hectares (5000 acres) of the Payette National Forest, and caused one injury. Data limitations in the West, including terrain-induced beam blockage, data voids due to large distances (≥ 200 km) between radars, and limited real time surface data, make severe weather decision making particularly challenging. Climatological records show that tornadic events in the Intermountain West are rare. Therefore, with limited data available for storm interrogation and the rarity of tornadic events within the region, proper pre-storm environmental analysis and utilization of available data sets throughout the event are especially crucial. This paper documents the pre-storm environment and the evolution of a tornadic cell through Bear, Idaho.

### 1. Introduction

On 4 June 2006, a quickly developing squall line swept across central Oregon and Idaho, which caused one injury and extensive damage to structures and the Payette National Forest. The southern portion of the line produced significant microburst damage across Baker and Adams counties, quarter-sized hail in Cuprum, Idaho, and an F2 tornado in Bear, Idaho.

Aerial surveys of the tornado damage, conducted by the Payette National Forest Service, revealed that approximately 2023 hectares (5000 acres) of timber were blown down, snapped in half, or uprooted. The path was 21 km (13 miles) long with a 0.8 km (0.5 miles) width in some locations (Fig. 2). Several houses in the small town of Bear, Idaho, where the tornado first touched down, suffered substantial roof damage. A storm survey of the damage along its path indicated that this tornado reached F2 intensity, with

winds of up to 69 $ms^{-1}$ (134 kt) (Fujita 1981). The last tornado that produced comparable damage was an F3 that struck Gooding County, Idaho, in April of 1940 (NCDC 2006).

Climate records from 1950 through 2006 indicate an average of three tornadoes are reported per year in Idaho, most of which are below F2 strength. Many of these reports come from the populated sections of the Snake River Valley (Fig. 3). While tornadoes likely occur over the higher terrain, many of these events are not seen or reported due to low population density.

Records from 1880 (Grazulis 1993) through the present indicate that no known tornadoes in Idaho history have reached F4 or greater strength. In addition, only two F3 tornadoes have been recorded. National Climatic Data Center (NCDC) records from 1950 through the end of April 2006 indicate nine tornadoes in Idaho have reached F2 strength. NCDC records also show an increase in reports over the past 50 years. This is likely due to an increase in population rather than strictly an increase in the occurrence of these events. In addition, developments in technology, such as the introduction of the WSR-88D, have also led to an increase in detection of severe events (Fujita et al. 1989).

The majority of Idaho tornado events occur in the late spring and summer during the late afternoon when surface instability is usually at its greatest. Tornadogenesis in the West is most often associated with non-supercellular storms. Most of these tornadoes are frequently referred to as “landspouts”. Landspouts develop during the early stages of convection in areas of strong low level instability where boundary layer vorticity is stretched into the updraft and tightened (Bluestein 1985).

Anticipating tornadic development is difficult, regardless of location. However, there are several complications in the West not seen in the central and eastern parts of the United States, which present additional challenges. Data available to a warning forecaster may be lacking in the West due to several factors, including radar beam blockage, high elevation radars, low population density, and a lack of observational equipment. Lower elevation angles from the WSR-88D radar are often blocked by terrain. This is especially problematic at longer distances from WSR-88D sites where storm structure frequently cannot be viewed below three kilometers (approximately 10000 ft) above ground level (AGL). Additional complications with respect to the utility of low level radar data arise when radars are placed at high elevation sites. Since the WSR-88D is not capable of viewing data below the 0.5º elevation angle, portions of storms that are located in valleys beneath this lowest slice can not be viewed, even at close distances to the radar. Using radar data from neighboring offices are not often advantageous due to the distance between radars. Over complex terrain, surface observation sensors are placed far apart as well. Furthermore, in sparsely populated areas, fewer “ground truth” reports from storm spotters are available (Fujita et al. 1989). Additionally, most of the existing storm spotters reside in the valleys.

Given that tornadic events in the West are rare, a warning meteorologist must carefully examine and understand the environment prior to event onset and monitor environmental changes over time. Potential impacts of terrain (Fig. 3) on the near storm

environment are also imperative to know. These impacts may enhance or decrease tornado potential.

## 2. Synoptic and Mesoscale Environment

On the morning of 4 June 2006, a negatively-tilted short wave trough at 500 mb moved across central Washington and Oregon (Fig. 4). A 500 mb vorticity maximum advected over central Oregon, with convection already developing ahead of this maximum as early as 1200 UTC. A 250 mb jet streak quickly moved northeast across Oregon, which would enhance lift in Baker County and the West Central mountains (Fig. 3). A northwest to southeast oriented 850 mb thermal ridge stretched across the Snake River valley ahead of the cold front. Previous studies in the northwestern United States (Evenson and Johns 1995) have shown that a 500 mb negatively tilted trough and a northwest to southeast oriented 850 mb thermal ridge are favorable conditions for a significant severe weather event.

Advanced Microwave Sounding Unit (AMSU) satellite data showed that precipitable water (PW) values were over 25 mm (one inch) off the Pacific Coast, while the 1200 UTC sounding at Boise showed 22.4 mm (0.88 inches), which was 160% of normal. Strong southwesterly flow of 25 $ms^{-1}$ (50 kt) at 500 mb ahead of the short wave trough enabled significant mid-level moisture advection over the higher terrain of the Owyhee and Seven Devil mountains along the Idaho and Oregon border.

Most locations in southeast Oregon and southwest Idaho reported surface dew point values between 8ºC (46ºF) and 12ºC (54ºF) throughout the morning (Fig. 5). Given sufficient instability and localized forcing, these dew point values typically support active deep convection in this area of the United States. Dew points in the area of interest remained between 10ºC (50ºF) and 14ºC (57ºF) throughout the event. The 1200 UTC sounding at Boise (KBOI) indicated 711 $Jkg^{-1}$ of Surface-Based CAPE (SBCAPE), while a lifted index of -3 ºC could be achieved at the time of maximum surface heating using a forecast maximum temperature of 29ºC (84ºF) and a dew point of 9ºC (48ºF). However, 1800 UTC NAM12 model data forecast that over 1500 $Jkg^{-1}$ of SBCAPE could be realized in association with the upper trough.

Modification of the KBOI sounding (Fig. 6) using an observed surface temperature of 16.1ºC (61ºF), a surface dew point of 13.9ºC (57ºF), expected cooling aloft, and lifting from 850 mb yielded greater understanding of the near storm environment. Using these values, a SBCAPE value near 2000 J/kg could be achieved. The environment was already favorable for hail formation with mid-level shear and a majority of the CAPE between 750 and 350 mb. Additionally, daytime heating in combination with the rapid cooling aloft associated with the passing upper trough would create very steep lapse rates later in the day, which would further increase the threat of large hail and strong downburst winds.

A veering wind profile and 0-6 km bulk shear values of 30-36 $ms^{-1}$ (60-70 kt) were also forecast in model data. Research by Thompson et al. (2003) has found that 0-6

km bulk shear values exceeding 20 $ms^{-1}$ (39 kt) typically support supercell formation in environments where deep convection develops. GFS40 and NAM12 data forecast an area of approximately 300 $m^2s^{-2}$ of 0-3km storm relative helicity (SRH) in Baker County by 1200 UTC, which would progress eastward through the day and diminish after 1800 UTC. Nearly 200 $m^2s^{-2}$ of 0-1 km SRH was forecast in this same area by the GFS40, while the NAM12 forecast nearly 300 $m^2s^{-2}$ over Baker County and the West Central mountains. The hodograph from 0-6 km showed a turning of the shear vector that would favor right moving supercells. Further analysis of the hodograph (Fig. 7) showed that an increase of southeasterly to southwesterly wind speeds, or backing of the low-level winds, would increase the SRH.

## 3. Storm Evolution

As the cold front progressed across central Washington and Oregon (Fig. 1), a squall line formed ahead of the boundary. By approximately 1605 UTC this line began to move into Baker County (Fig. 8). Radar limitations at this distance and over complex terrain affected storm interrogation. The southern end of the squall line was located 213 km (115 nm) from the radar and the lowest slice, 0.5º, was sampling at four km (approximately 13100 ft) AGL. Therefore, the evolution of the lowest portions of the storm below this elevation could not be detected by radar.

Storm relative velocity data at 1605 UTC from the KCBX radar at the 0.5º elevation angle indicated 15 $ms^{-1}$ (30 kt) of mid-level rotation, while storm structure shown from reflectivity data may have been unrepresentative of the severity (Fig. 9). Reflectivity cores were less than 50 dBZ at the freezing level of approximately 3.7 km (12100 ft) above sea level (ASL) and above. The strongest reflectivities of the storm (approximately 45 dBZ at 4.3 km, or 14.2 kft) were located in the valley near Sumpter, Oregon. At 1630 UTC, two separate calls from trained spotters in this location revealed that the line was producing estimated winds of 27$ms^{-1}$ (52 kt) and 1.9 cm (0.75 inch) hail.

By 1650 UTC a rear-inflow notch (RIN) and bow echo were apparent, supporting spotter reports of severe winds (Fig. 10). Surface winds were still from a southeasterly to southerly direction while the Velocity Azimuth Display (VAD) wind profile at KCBX showed an increase in speeds of southwesterly winds just above the surface, which supported increased helicity. Velocity data revealed a tightening couplet in the mid levels of the storm.

By 1717 UTC, reflectivity data suggested increasing probability of large hail with 60 to 65 dBZ cores at 3.9 km (12900 ft) AGL, and 55 to 60 dBZ cores at 6.4 km (21100 ft) AGL (Fig.11). Outbound velocities at the 0.5º level had increased to nearly 15 $ms^{-1}$ (30 kt) while storm top divergence had increased to 36 $ms^{-1}$ (70 kt). Around this time, a Remote Automated Wind Sensor (RAWS) station at Flagstaff Hill, approximately 16 km (10 miles) East of Baker City, measured a wind gust of 36 $ms^{-1}$ (70 kt).

By 1734 UTC, reflectivity cores of 60 to 65 dBZ (Fig.12) were observed at 7.3 km (24000 ft) and implied increased severity. The 50 dBZ core extended to nearly 9.1 km

(29900 ft). At this point the mean wind was from 230º at 18 $ms^{-1}$ (35 kt), while the storm began to deviate to the right of the mean wind with a motion of 260º.

By 1739 UTC, outbound velocities at the 0.5º level increased to nearly 21 $ms^{-1}$ (40 kt) and expanded in area (Fig.13). Storm top divergence increased to 41 $ms^{-1}$ (80 kt). The storm maintained this magnitude of storm top divergence over the next hour. A damaging downburst was soon reported by a spotter located 16 km (10 miles) north of Halfway, Oregon.

By 1805 UTC, outbound velocities at the 0.5º level again increased with speeds near 26 $ms^{-1}$ (50 kt). The storm began to show an increase in rotational velocities while strong outbound velocities of 26 $ms^{-1}$ (50 kt) had been maintained (Fig.14). The VAD wind profile at KCBX showed that wind speeds had increased and veered from a south to southwest direction (Fig. 15). The Snake River RAWS site (SRFI1) from a valley located in Hells Canyon approximately 13 km (8 miles) to the east of the storm indicated surface winds from the southeast, which would create a veering profile ahead of the storm. Adjusting the hodograph with the Mesonet and VAD winds more than doubled the SRH to 250 $m^2s$, and indicated increased tornado potential. The storm approached a northwest to southeast oriented portion of Hells Canyon, where it is possible that the observed low level southeasterly winds could channel moisture through the Canyon (Monteverdi et al. 2003). If this occurred, then this moisture advection likely increased the buoyancy within this local environment which enhanced the severity of the storm.

As the storm moved over Hells Canyon around 1809 to 1814 UTC, the detected rotation appeared to weaken. However, outbound velocities remained strong (Fig.16), and for the first time in the storm's existence, 50 to 55 dBZ cores extended up to 10.4 km (~ 34000 ft) (Fig.17). From here the storm progressed quickly. At 1827 UTC, the storm displayed a clear RIN and rotational velocities jumped up to 21 $ms^{-1}$ (40 kt) (Fig.18). Within the next few minutes tornadogenesis occurred, and rotational velocities increased to 23 $ms^{-1}$ (45 kt). Eyewitness reports in Bear, Idaho, indicated the tornado touchdown time was near 1830 UTC. Quarter sized hail was also reported from Cuprum, Idaho. Ten minutes after touchdown, the storm finally began to weaken.

## 4. Summary and Conclusions

In the Bear, Idaho tornado case, environmental analysis showed that conditions were favorable for damaging winds, large hail, and tornado formation. Utilizing a variety of available datasets, a forecaster could continue to evaluate how this near-storm environment progressed and continued to support severe potential.

In this case, Mesonet data showed that dew points remained high while temperatures increased. VAD wind profile data showed an increase in south to southwest winds, and an increase in southeasterly winds at the surface ahead of the storm, which increased the SRH.

Although radar data were unavailable beneath three kilometers (approx. 10000 ft), there were indications of the storm's increasing severity. Persistent rotation in storm-relative motion (SRM) and base velocity data and continual ground truth reports of severe weather indicated that the storm was maintaining strength. The storm was relatively unimpeded by rough terrain as it traversed across a valley. An increase in storm inflow and a rapid increase in reflectivity values were noted shortly before the cell became tornadic as the storm passed over Hell's Canyon.

Examining these important near-storm environmental clues where data sources are limited proved to be vital in this severe weather episode. By utilizing all datasets and keeping a constant state of awareness of how the environment is evolving, a forecaster can use the information available to make better warning decisions.

**Acknowledgements**

The author would like to thank Peter Wolf, Angela Lese, Jon Zeitler, and Randy Graham for their constructive criticism and valuable insights into this case. The author would also like to thank Angela Enyedi, Dan Miller, Jay Breidenbach, George Skari, and Charles Redman for their helpful insights as well. Thanks to Timothy Barker for archiving and providing data for this case. Much gratitude goes to the Boise and Jacksonville WFOs for providing education, opportunity, guidance, and countless hours of entertainment on shift.

**References**

Bluestein, H.B., 1985: The formation of a "landspout" in a "broken-line" squall line in Oklahoma. *Preprints, 14th Conf. on Severe Local Storms,* Indianapolis, 267-270.

Evenson, E.C., and R.H. Johns, 1995: Some Climatological and Synoptic Aspects of Severe Weather Development in the Northwestern United States. *National Weather Digest*, 20, 1, 34-50.

Fujita, T.T., 1981: Tornadoes and downbursts in the context of generalized planetary scales. *J. Atmos. Sci.*, **38**, 1511-1634.

1989: The Teton-Yellowstone Tornado of 21 July 1987. *Mon. Wea. Rev.,* **117**, 1913-1940.

Grazulis, T. P., 1993: *Significant Tornadoes 1680–1991.* Environmental Films, 1326 pp.

Monteverdi, J.P., C.A. Doswell, G.S. Lipari, 2003: Shear Parameter Thresholds for Forecasting Tornadic Thunderstorms in Northern and Central California. *Mon. Wea. Rev.*, 18, 357-370.

NCDC, 2006: *Storm data.* Vol. 48, No. 5.

Thompson, R.L., R. Edwards, J. Hart, K.Elmore, and P. Markowski, 2003: Close Proximity Soundings within Supercell Environments Obtained from the Rapid Update Cycle. *Weather and Forecasting*, 18, 6, 1243-1261.

Wakimoto, R., and J.W. Wilson, 1989: Nonsupercell tornadoes. *Mon. Wea. Rev.*, **117**, 113-1140.

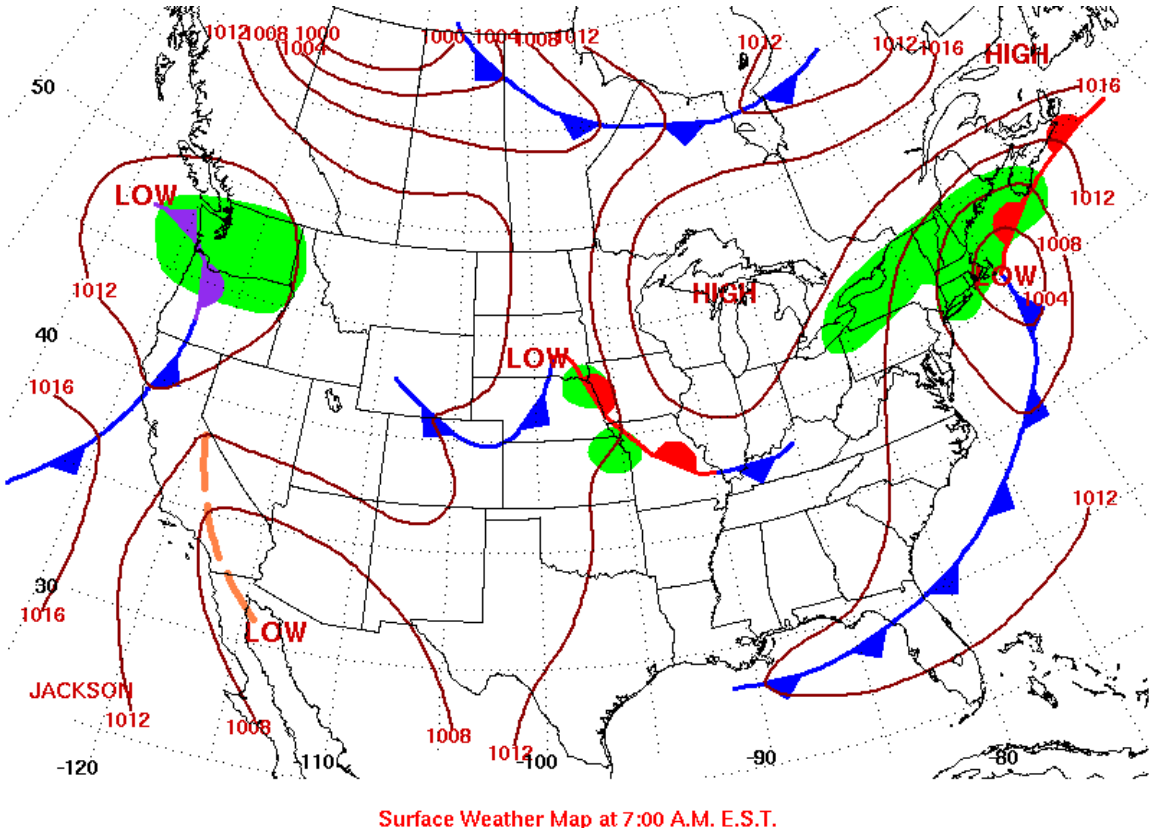


Fig 1: Hydrometeorological Prediction Center (HPC) surface analysis on 4 Jun 2006 at 1300 UTC showing cold front moving into the Pacific Northwest.

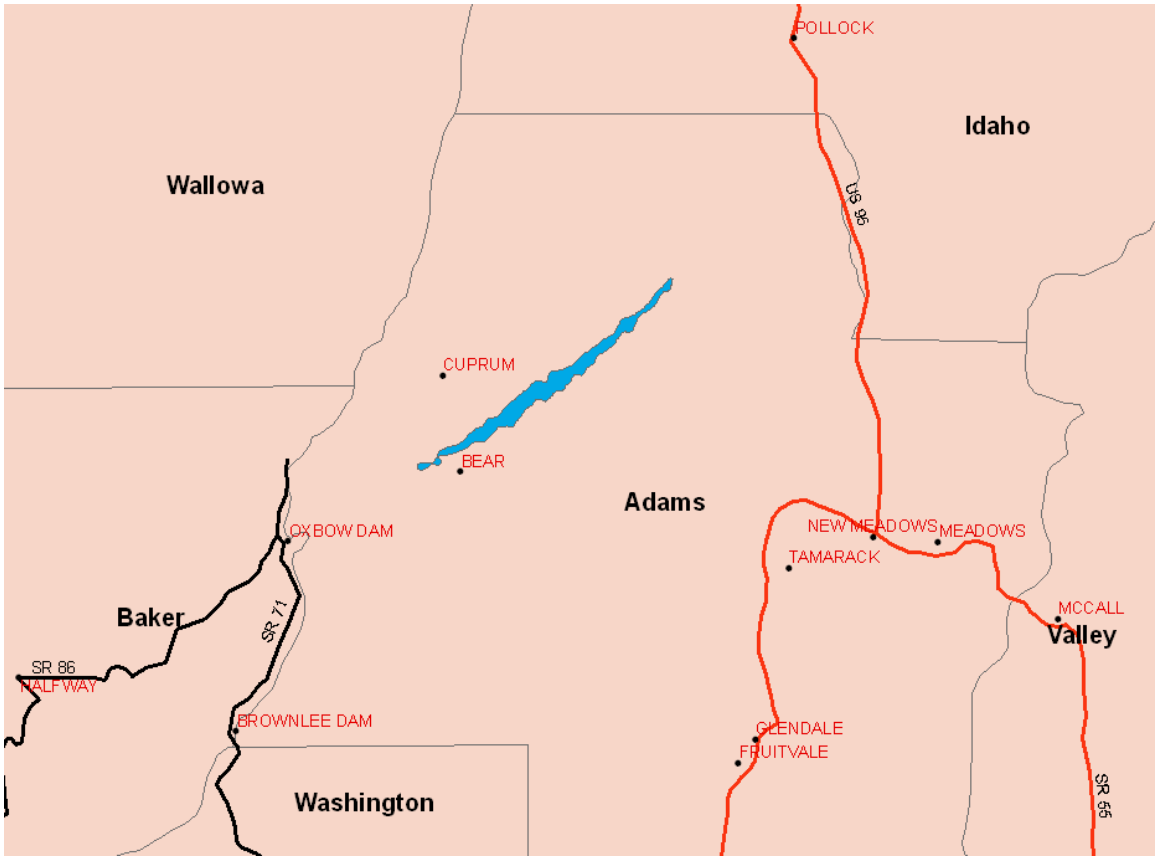

Fig 2: Tornado path (blue) through Adams County, Idaho, on 4 Jun 2006.

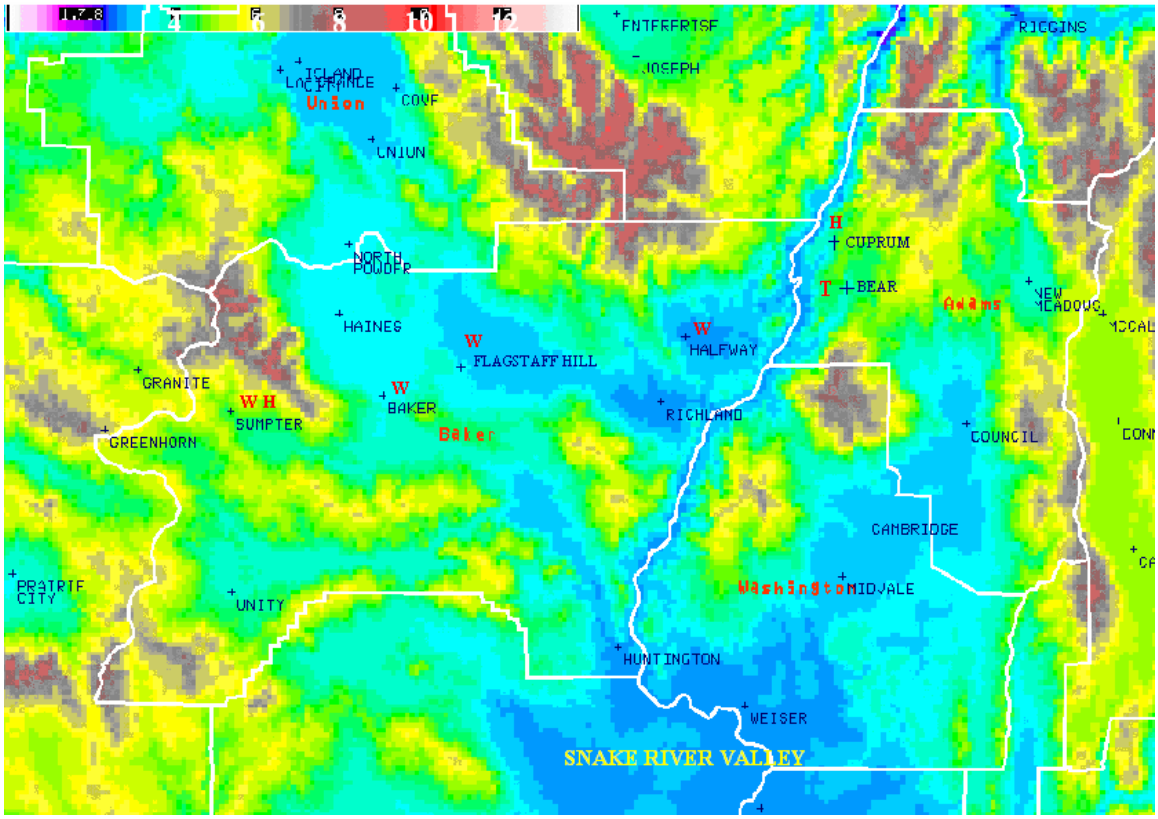


Fig 3: High resolution topography image including storm reports. Scale at the top is in kft. W represents wind reports, H represents hail reports, and T represents the location of tornado touchdown on 4 Jun 2006. County names are in red and city names are in blue. Only the extreme northwestern portion of the Snake River Valley is shown.

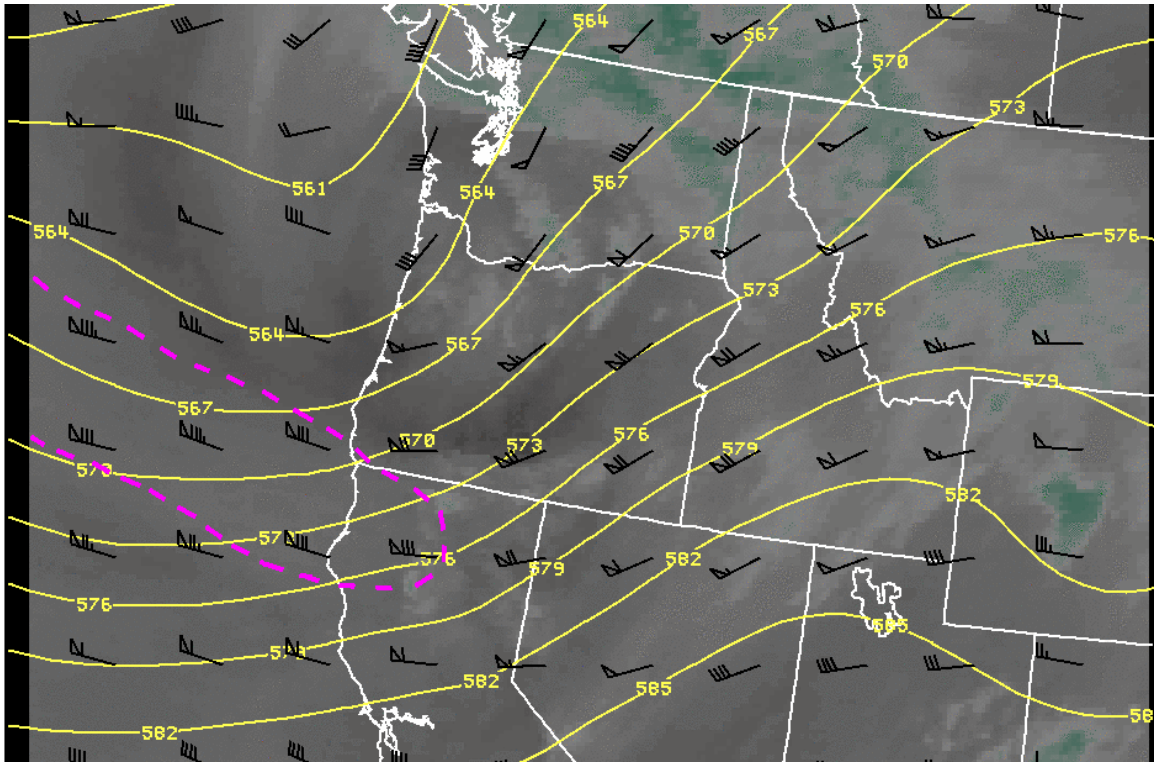

Fig 4: 1200 UTC 4 Jun 2006 water vapor image with 500 mb heights and 250 mb winds overlaid. The pink dashed line represents the 41 $ms^{-1}$ (80 kt) isotach, showing the position of the wind maximum.

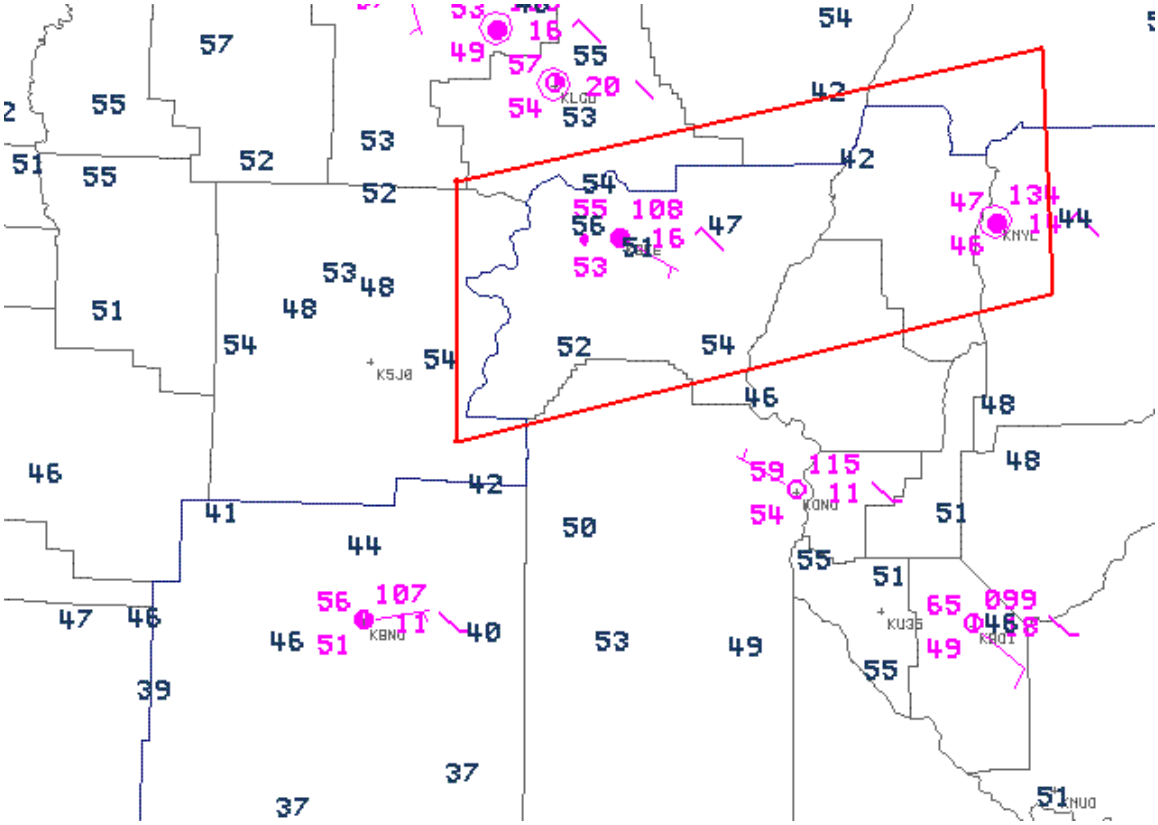

Fig 5: 1200 UTC 4 Jun 2006 ASOS plot, shown in pink, (temperature and dew point temperature in ºF) and Mesonet dew point temperatures (ºF), shown in blue. The area of interest is outlined in red.

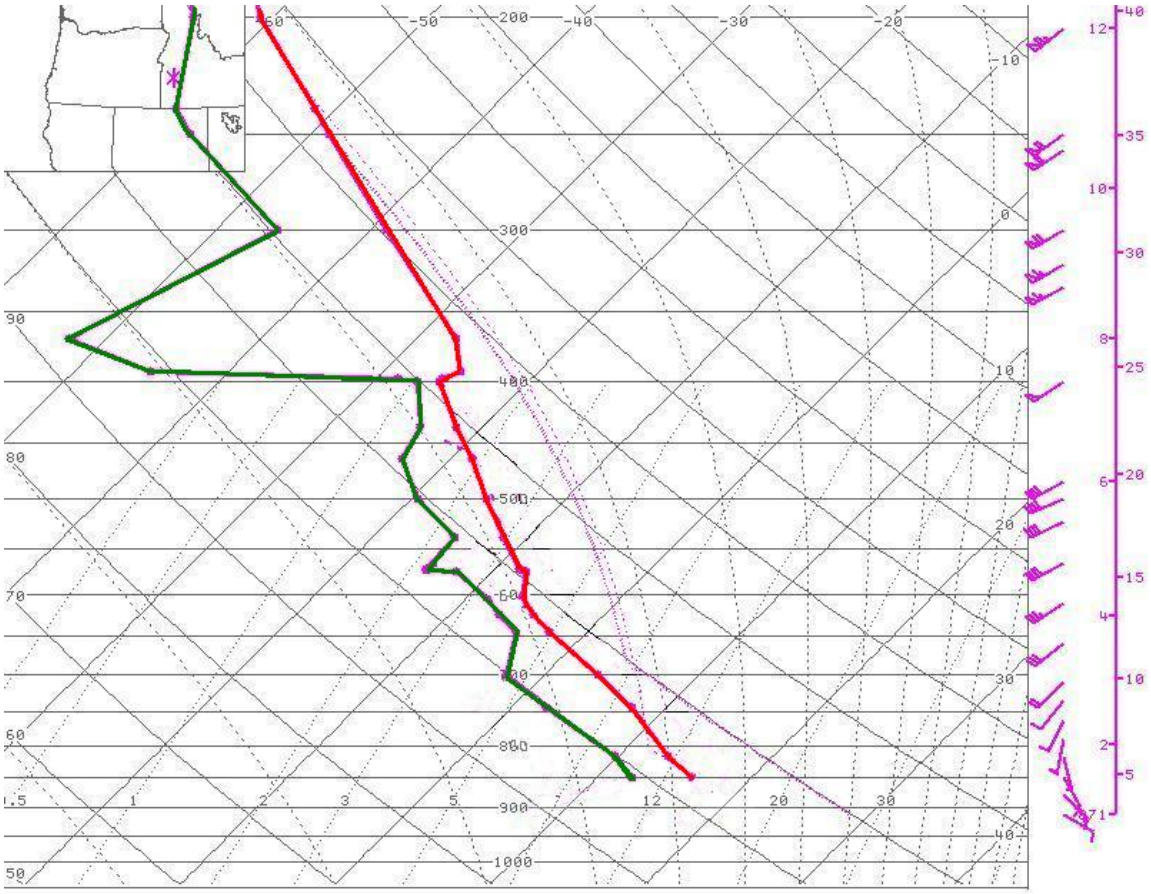

Fig 6: Modified 1200 UTC 4 Jun 2006 sounding at KBOI, lifting from 850 mb.

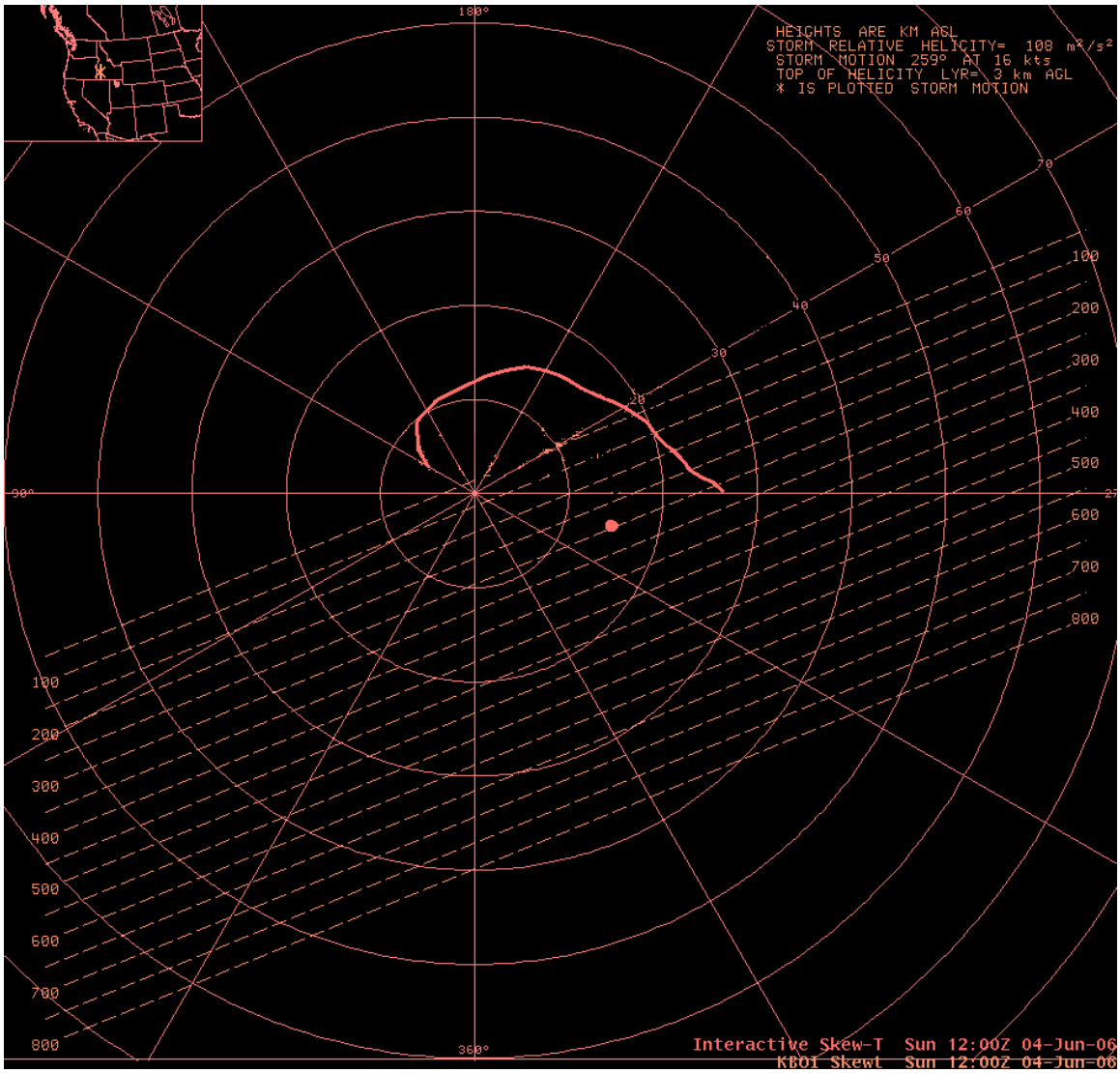

Fig 7: 1200 UTC 4 Jun 2006 hodograph at KBOI modified with VAD winds at 1815 UTC.

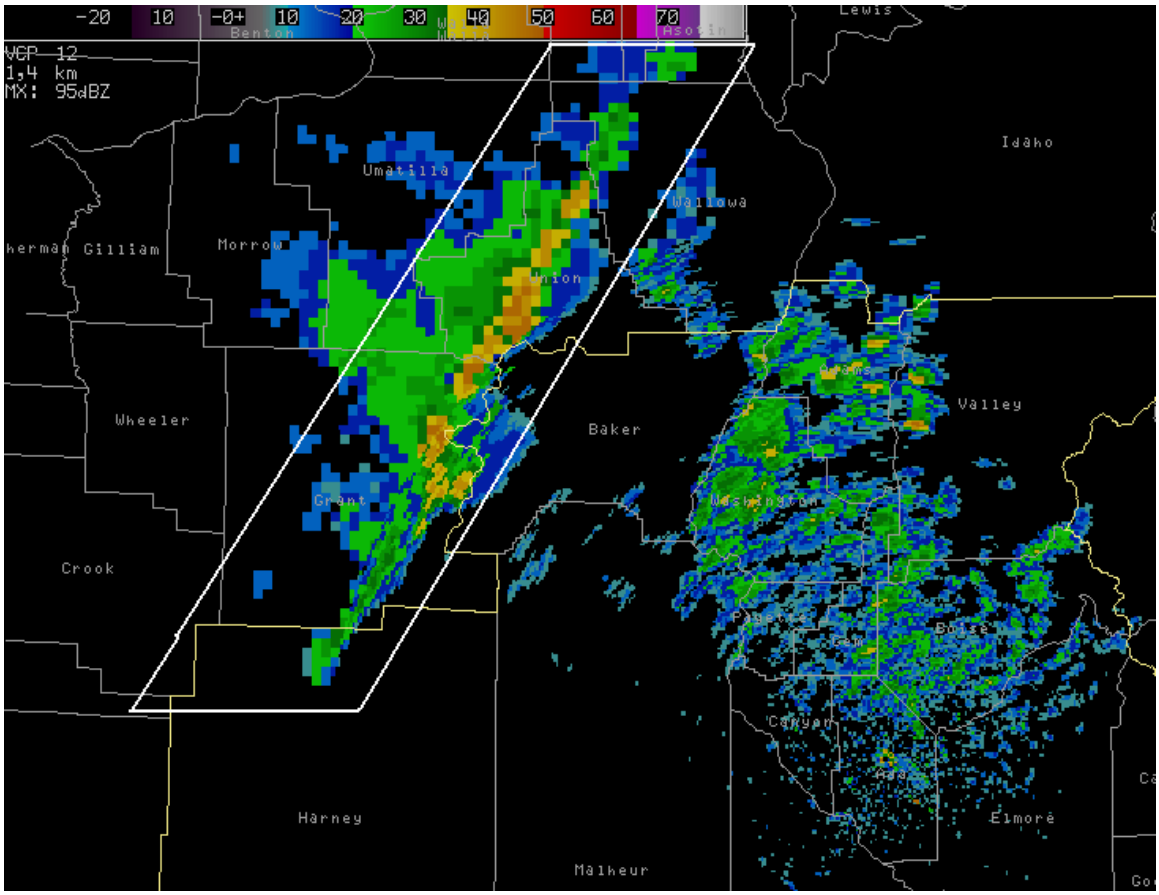

Fig 8: KCBX composite reflectivity of the squall line (white polygon) moving into Baker County at 1605 UTC on 4 Jun 2006.

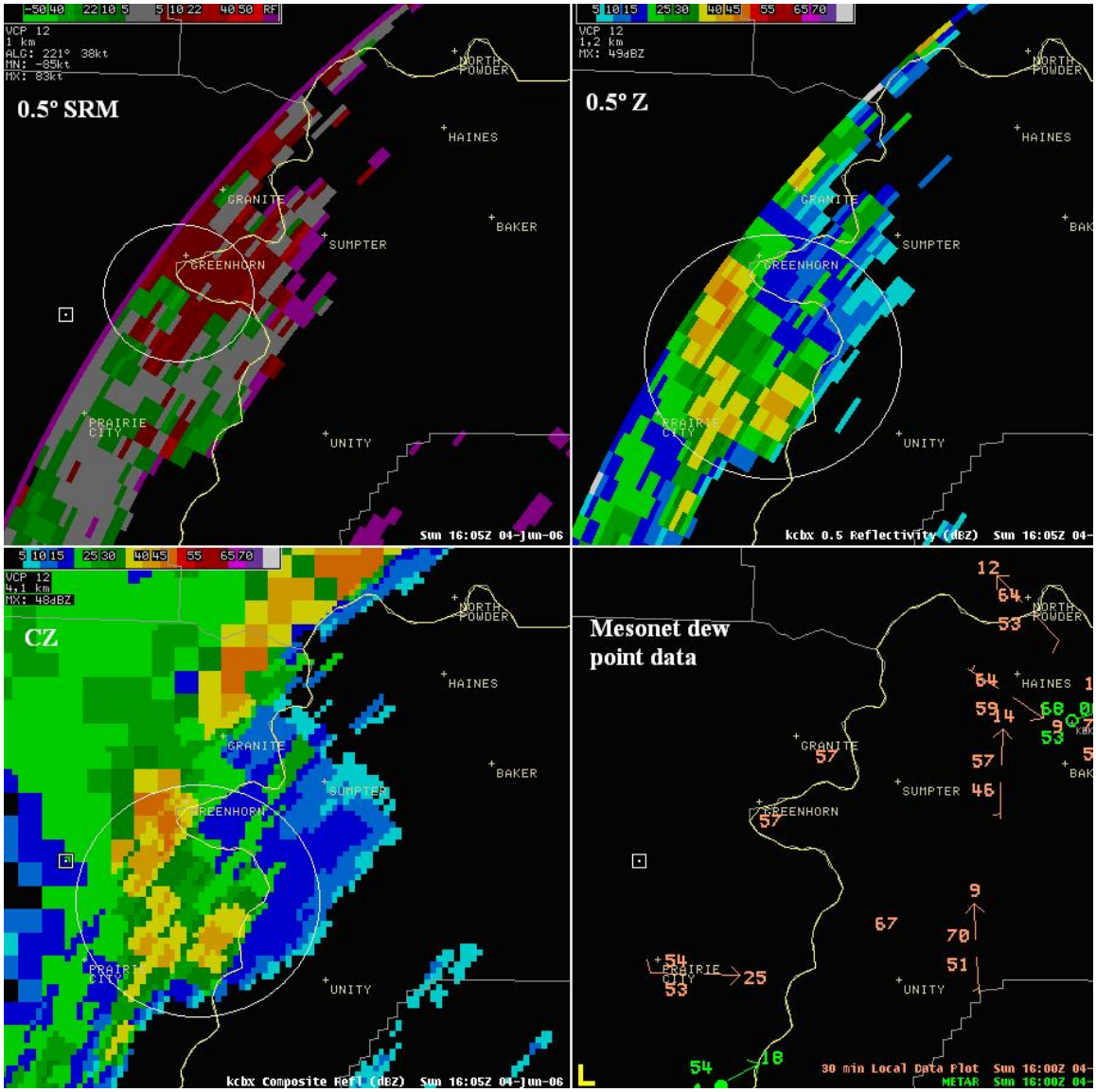


Fig 9: 1605 UTC 4 Jun 2006 showing KCBX 0.5º SRM, 0.5º reflectivity, Mesonet dew point data (shown in orange), and composite reflectivity. The area of interest is encircled in white. KCBX is located southeast of the squall line, and 222 km (120 nm) from the cell of interest.

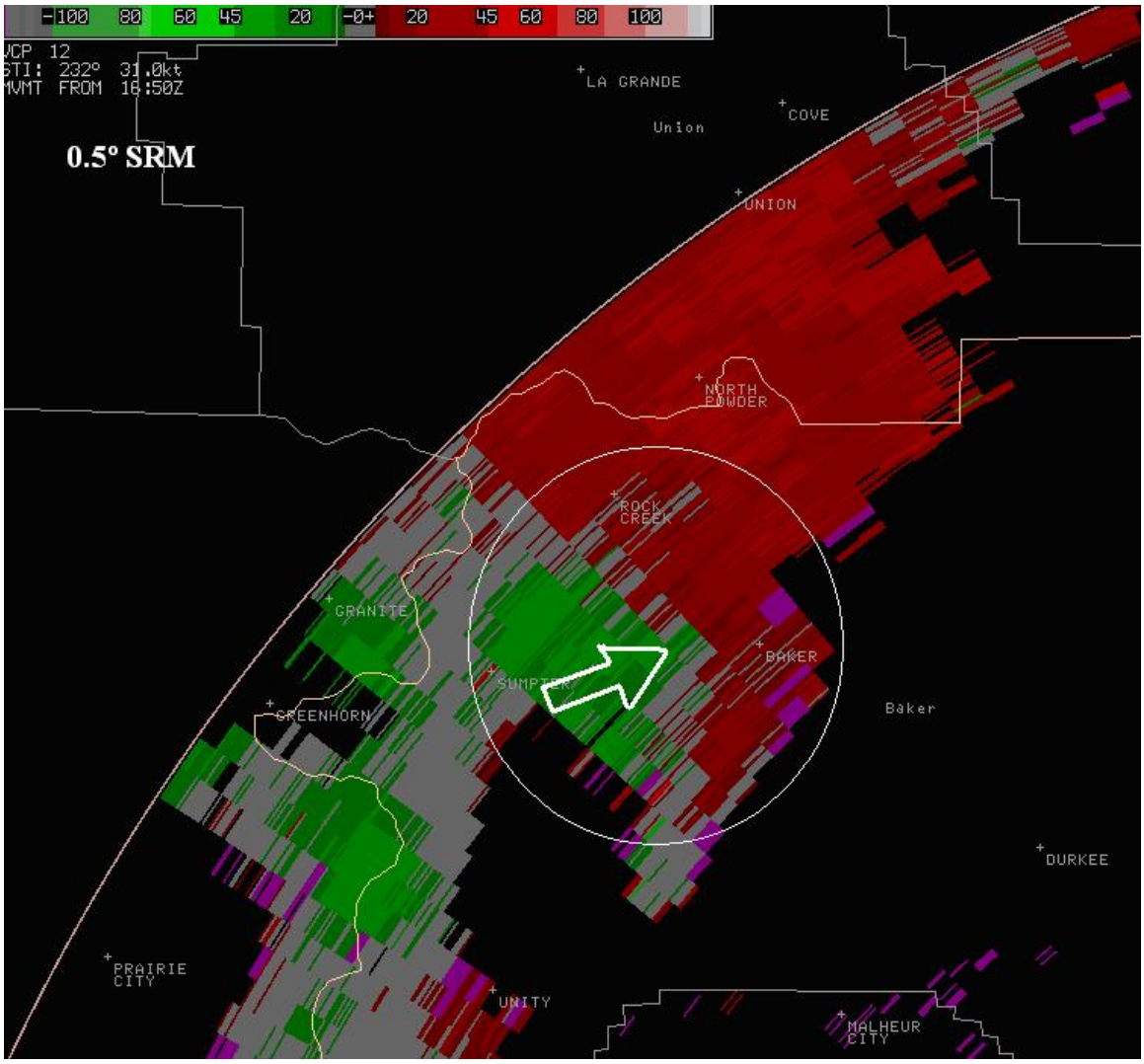

Fig 10: KCBX 0.5º SRM image at 1650 UTC 4 Jun 2006 showing the RIN (arrow) and a tightening rotation. The center of the cell is located 189 km (102 nm) from KCBX.

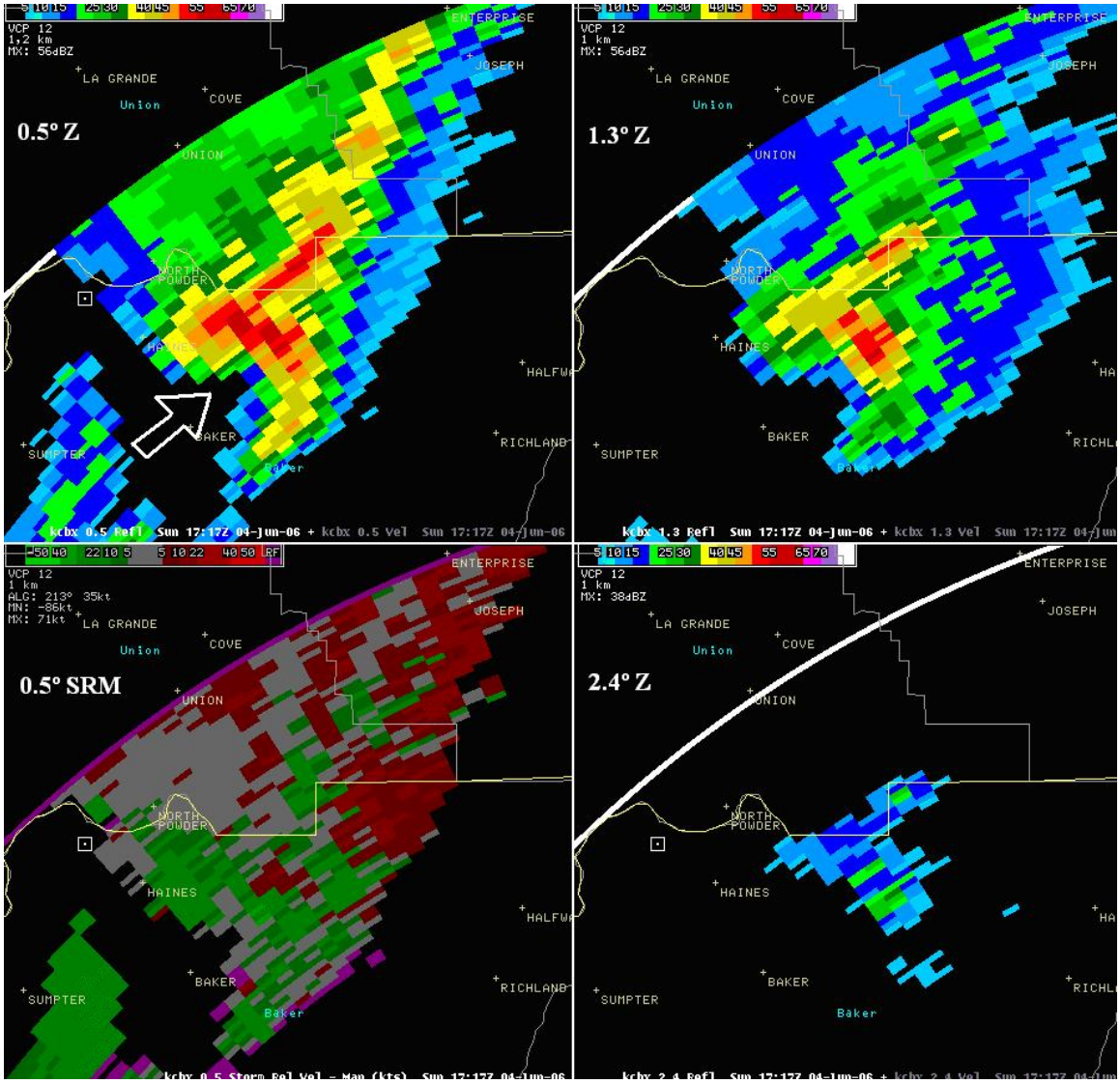


Fig 11: 1717 UTC 4 Jun 2006 displaying the RIN (arrow) and increase in reflectivities. Shown are the KCBX 0.5º, 1.3º, and 2.4º reflectivities, and the 0.5º SRM. The center of the cell is located 192 km (104 nm) from KCBX.

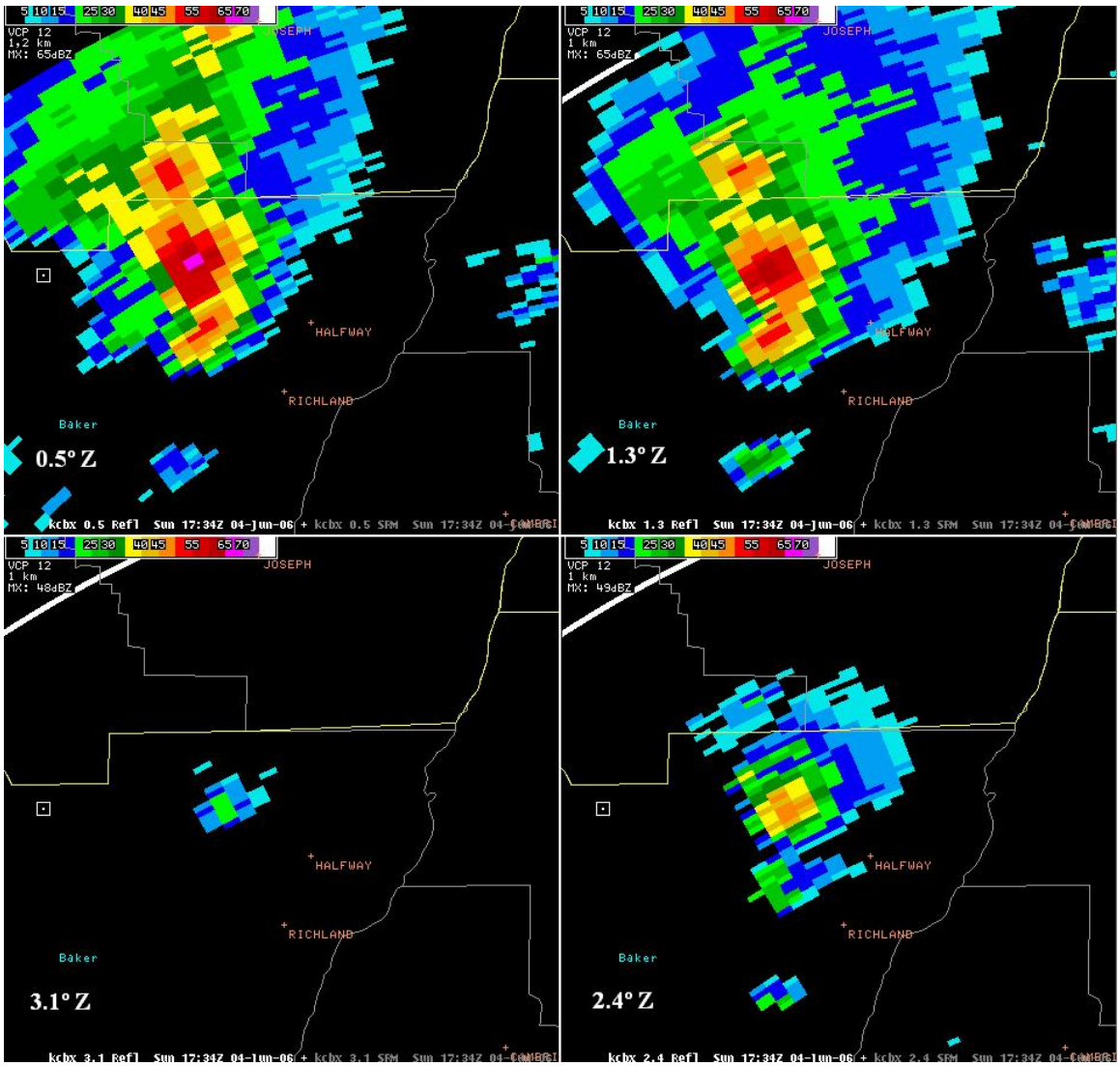

Fig 12: 1734 UTC 4 Jun 2006 KCBX 0.5º, 1.3º, 2.4º, and 3.1º slices, displaying an increase in reflectivities. The center of the cell is located 187 km (101 nm) from KCBX.

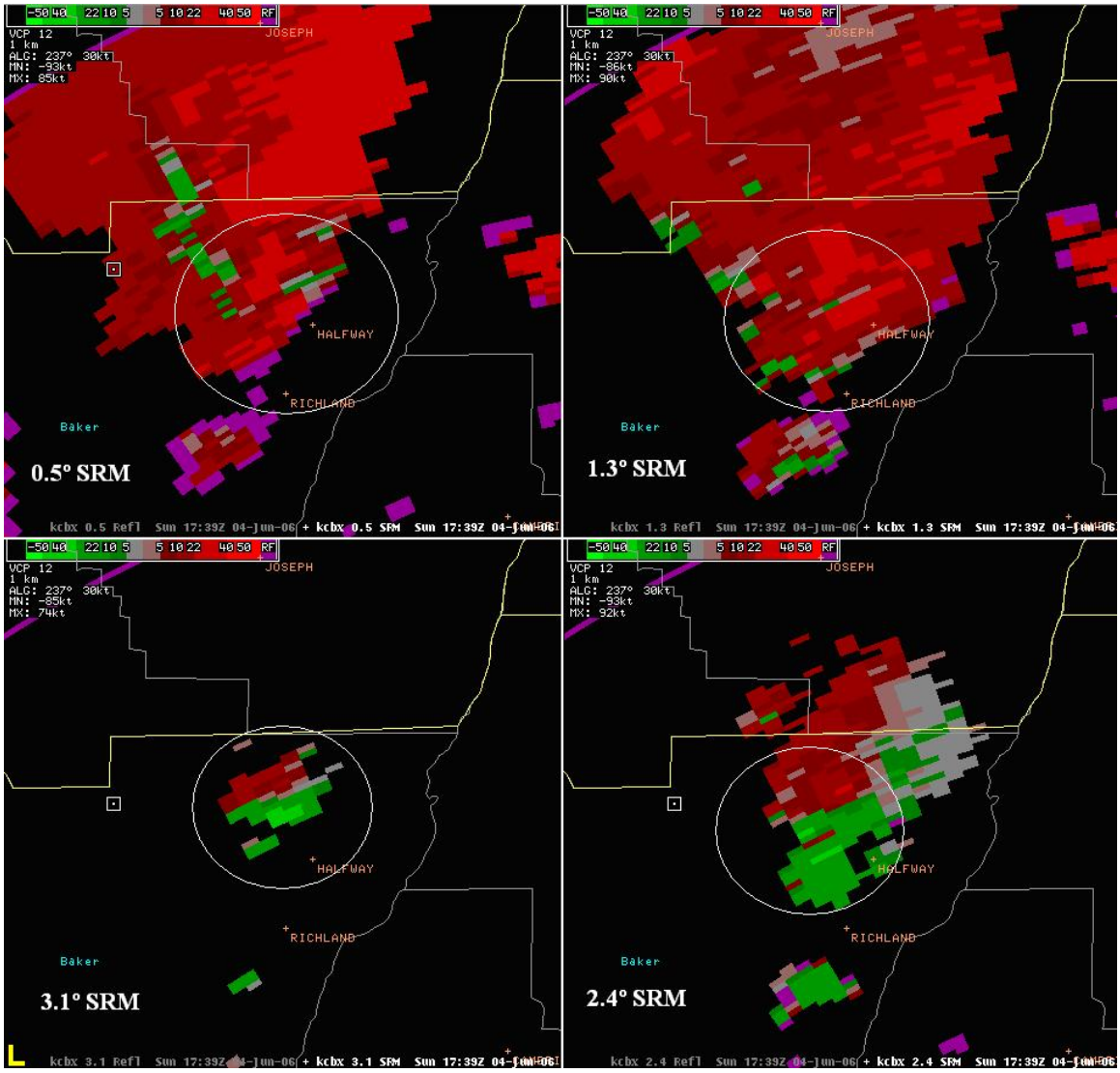

Fig 13: 1739 UTC 4 Jun 2006 KCBX 0.5º, 1.3º, 2.4º, and 3.1º SRM showing a large area of strong outbound velocities and increased storm top divergence, which are encircled in white. The center of the cell is located 187 km (101 nm) from KCBX.

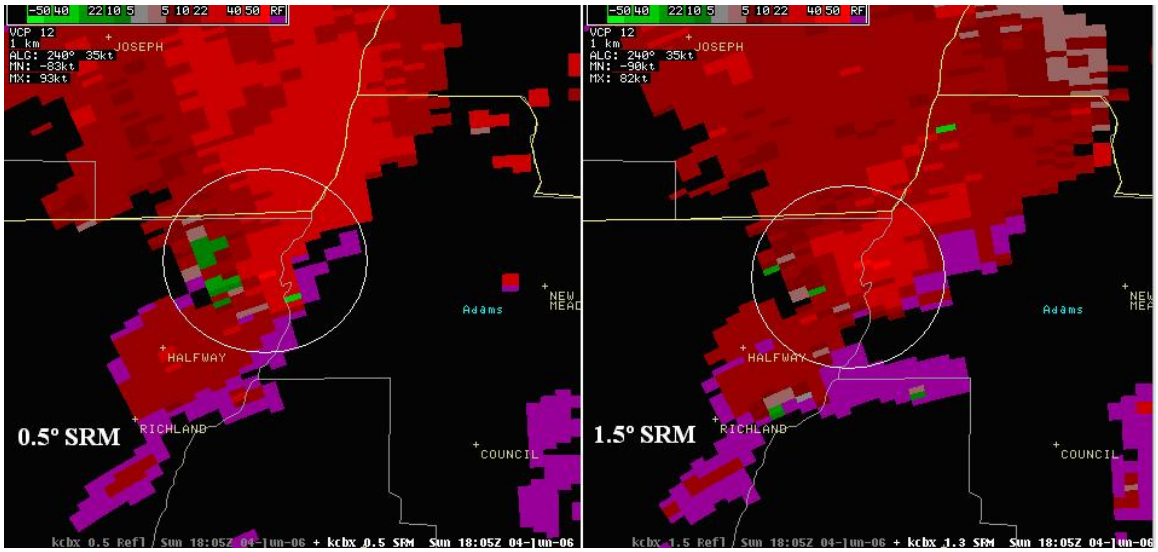

Fig 14: 1805 UTC 4 Jun 2006 KCBX 0.5º and 1.5º SRM showing an increase in rotational velocities, which is encircled in white. The center of the cell is located 180 km (97 nm) from KCBX.

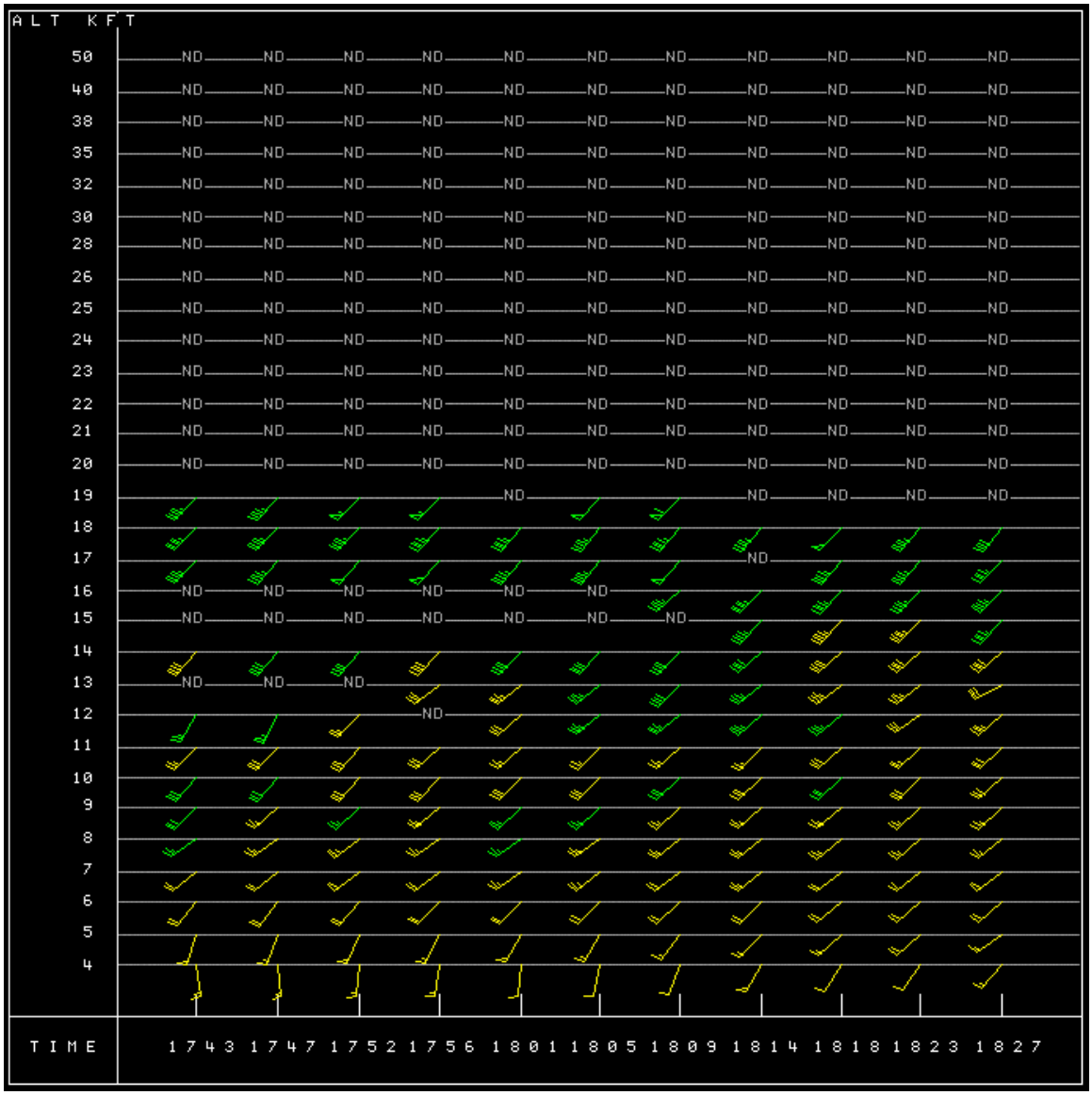

Fig 15: KCBX VAD wind profile from 1743 UTC through 1827 UTC 4 Jun 2006 showing an increase in south to southwest winds.

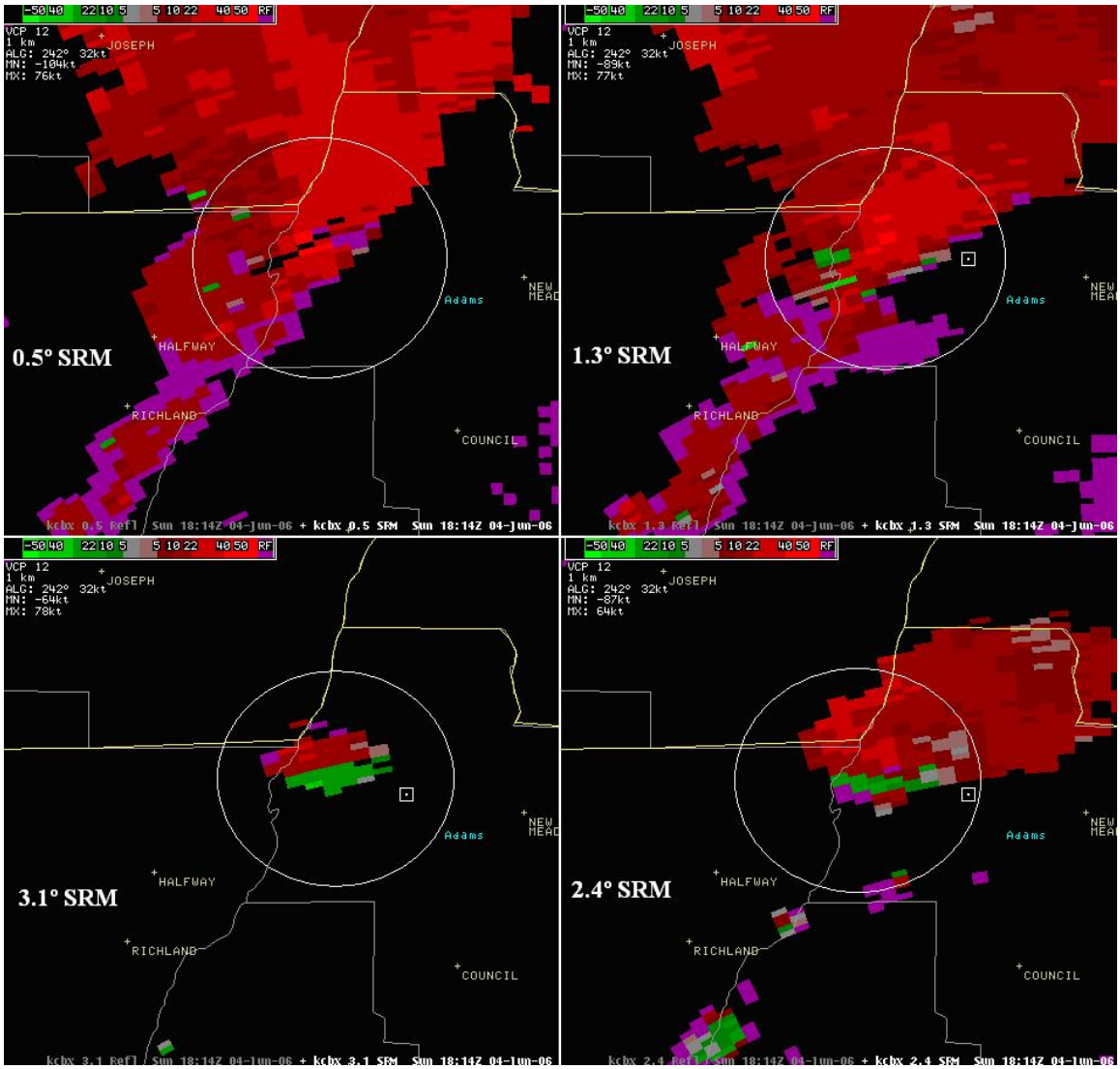

Fig 16: 1814 UTC 4 Jun 2006 KCBX 0.5º, 1.3º, 2.4º, and 3.1º SRM showing increased outbound velocities and storm top divergence, which are outlined in white. The center of the cell is located 180 km (97 nm) from KCBX.

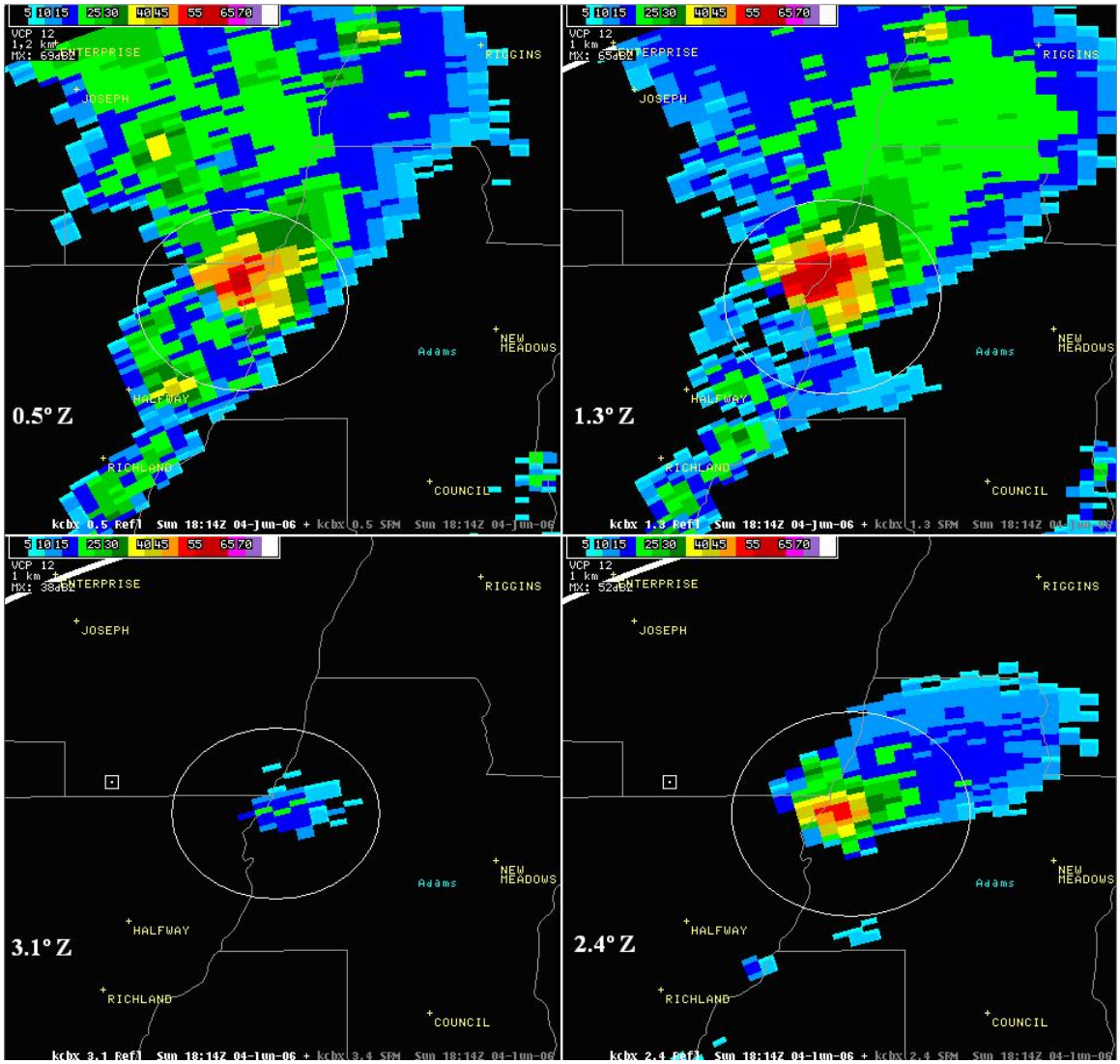

Fig 17: 1827 UTC 4 Jun 2006 KCBX display of 50 to 55 dBZ cores extending up to 10.4 km. The center of the cell is located 181 km (98 nm) from KCBX.

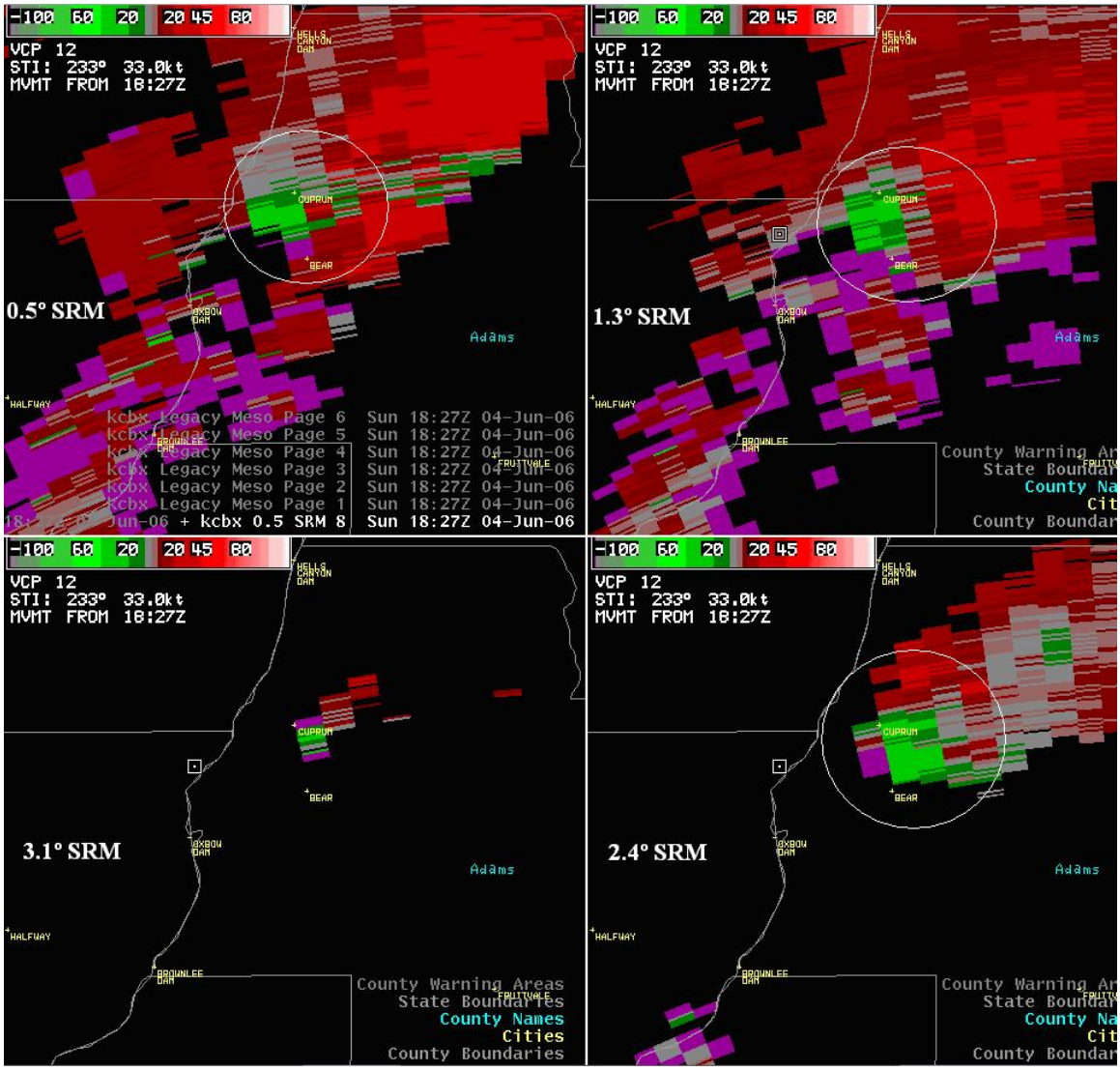

Fig 18: 1827 UTC 4 Jun 2006 KCBX 0.5º, 1.3º, 2.4º, and 3.1º SRM showing a rapid increase in rotational velocity. The center of the cell is located 181 km (98 nm) from KCBX.